Biomaterials Science

ROYAL SOCIETY OF CHEMISTRY

PAPER

View Article Online
View Journal | View Issue

Cite this: *Biomater. Sci.*, 2021, **9**, 4308

Effect of polymeric excipients on nucleation and crystal growth kinetics of amorphous fluconazole†

Jie Zhang,‡ Zhengyu Liu,‡ Haomin Wu and Ting Cai *

Amorphous solids have been widely used to improve the solubility and oral bioavailability of poorly water-soluble drugs. Biocompatible polymeric materials are usually incorporated into formulations to inhibit the crystallization of high-energy amorphous drugs. Crystallization typically consists of two steps, nucleation and crystal growth. The impacts of polymeric excipients on the crystal growth of amorphous drugs have been intensively studied. However, the nucleation behaviors of amorphous drugs in the presence of polymers remain largely unexplored. Herein, we report that three chemically distinct polymers show significantly different effects on nucleation kinetics of amorphous fluconazole (FCZ), a classical antifungal drug. The addition of 10% w/w HPMCAS shows the largest inhibitory effect on the nucleation rates of FCZ, while the same amount of PVP has only a minor effect. Conversely, the nucleation rates for both polymorphs of FCZ are significantly increased in the presence of PEO. In addition, the polymeric additives are found to influence the kinetics of nucleation and crystal growth to a similar extent, suggesting that the two processes may share a similar kinetic barrier. The present study is helpful in the optimization of formulations of amorphous solid dispersions and understanding the nucleation behavior of polymorphic drugs.

Received 20th January 2021,
Accepted 11th February 2021

DOI: 10.1039/d1bm00104c

rsc.li/biomaterials-science

Introduction

Using amorphized pharmaceuticals in solid oral dosage forms has received increasing attention because amorphous solids can often provide enhanced solubility, dissolution rate and bioavailability for poorly soluble drugs.[1,2] However, high free-energy amorphous drugs would have the risk of recrystallization over time and consequent loss of therapeutic efficacy.[1,2] Thus, maintaining the physical stability of amorphous drugs is crucial for developing robust formulations.

Amorphous drugs are usually formulated with biocompatible polymeric excipients, forming amorphous solid dispersions to achieve enhanced physical stability. Several mechanisms have been proposed to interpret the impact of polymeric excipients on the stability of amorphous drugs.[3,4] The hydrogen-bonding interactions between polymers and drugs have been demonstrated to enhance the physical stability of amorphous drugs by reducing their molecular mobilities.[5,6] Some other types of molecular interactions such as ionic, dipole–dipole, and van der Waals interactions were also reported to play important roles in inhibiting the crystallization of amorphous drugs.[7,8] However, different polymeric carriers might have different impacts on the stability of amorphous drugs. Rather than inhibiting crystallization, low-concentration poly (ethylene oxide) (PEO) could significantly accelerate the crystal growth rates of amorphous drugs by orders of magnitude.[9–12] Recently, Yu and co-workers proposed a model in which the impact of a polymer on crystallization kinetics of an amorphous drug was governed by the segmental mobility of the polymer.[13]

Crystallization of amorphous materials typically consists of two steps, nucleation and crystal growth. Much attention has been focused on the impact of additives on crystal growth. However, the nucleation step could also be the crucial factor in governing the physical stability of amorphous pharmaceuticals. For instance, Taylor and co-workers found that the inhibitory effect of hydroxypropyl methylcellulose (HPMC) on the nucleation of amorphous felodipine determined the kinetics of the overall crystallization process.[14] However, the nucleation of amorphous drugs is still not well understood, and the effects of additives on the nucleation process are quite controversial in the literature.[15–17] For example, poly(acrylic acid) (PAA) was found to increase the nucleation rates of acetaminophen, while hydroxypropyl methylcellulose acetate succinate (HPMCAS) exhibited a strong inhibitory effect on nucleation rates.[16] In another study, three polymers, poly(vinylpyrrolidone) (PVP), HPMCAS, and HPMC, exhibited comparable effects in decreasing the nucleation rate of felodipine.[18] In the study of the effect of additives on nucleation kinetics of amor-

State Key Laboratory of Natural Medicines, Department of Pharmaceutics, School of Pharmacy, China Pharmaceutical University, Nanjing 210009, China. E-mail: tcai@cpu.edu.cn; Tel: +86-025-83271123

†Electronic supplementary information (ESI) available. See DOI: 10.1039/d1bm00104c

‡These authors contributed equally to this work.

phous flutamide, six polymers had only a minor effect on the nucleation rates, while a structural analog, nilutamide, significantly inhibited the nucleation. Recently, Yu and co-worker found that PVP can slow the crystal nucleation and growth of D-sorbitol and D-arabitol to a similar extent, suggesting that the nucleation and growth process might share a similar kinetic barrier and the polymeric additive acts as a mobility modifier to influence the two mobility-limited processes.[19]

Understanding the effects of polymeric additives on nucleation kinetics of the drug is of importance in the rational design of amorphous formulations with superior physical stability. In this work, we use fluconazole (FCZ) as a model compound to further explore the effects of polymeric additives on nucleation and crystal growth. FCZ is a classical antifungal drug that has low aqueous solubility.[20,21] The nucleation and crystal growth rates of FCZ are measured as a function of the temperature and polymer content. In addition, we compare the impact of polymeric additives on the nucleation and crystal growth kinetics of two FCZ polymorphs.

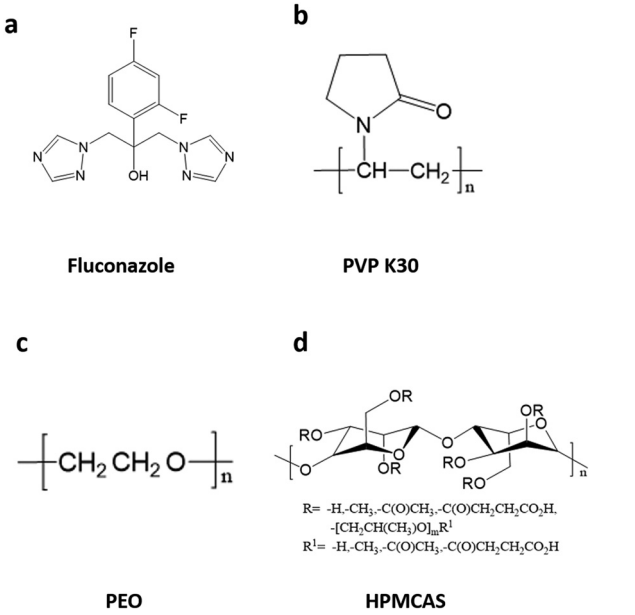

Fig. 1 Chemical structures of FCZ (a) and the repeating monomer units of PVP K30 (b), PEO (c) and HPMCAS (d).

Materials and methods

Materials

Fluconazole (FCZ) (purity > 99.0%, Form I) was purchased from Aladdin. Poly(ethylene oxide) (PEO, M_v = 100 000) was obtained from Sigma-Aldrich and used as received. Hydroxypropyl methylcellulose acetate succinate (HPMCAS-LF, M_v = 55 000–93 000) was obtained from Ashland and used as received. Polyvinyl pyrrolidone (PVP K30, M_v = 44 000–54 000) was obtained from BASF and dried in a vacuum drying oven at 343 K for 4 h before using. The chemical structures of FCZ and polymeric excipients are shown in Fig. 1. The physical properties of the drug and polymeric excipients are shown in Table S1.†

Methods

Preparation of FCZ/polymer binary physical mixtures. The physical mixtures containing 2.5%, 5%, 10%, 20% and 30% w/w polymers were prepared by mixing the corresponding amount of drugs and polymers using a mortar and pestle.

Measurement of nucleation rates. A two-stage method was applied to measure the nucleation rates.[19,22] In brief, the nuclei were initially formed at a low temperature, and then the sample was quickly switched to an elevated temperature to allow the nuclei to grow to visible dimensions under a polarized microscope. In this study, amorphous drugs or amorphous solid dispersions were prepared by melting 3–5 mg of crystalline powder between two coverslips at 423 K (12 K above the melting point of FCZ Form I) for 5 min on a hot stage (Linkam, THMS 600). The resulting liquid film was rapidly quenched to the desired temperature at 100 K min^{-1} and isothermally annealed for a given time to nucleate. The annealed sample was then heated to 373 K at a heating rate of 100 K min^{-1}, allowing the nuclei to grow up to crystals with visible sizes. The number of crystals was counted under a polarized light microscope (Olympus, BX53). For each sample, at each time point, a total of 20 images were recorded. The reported nucleation rate was the average of 20 measurements in 3 independent samples.

Measurement of crystal growth rates. The crystal growth rate was determined by tracking the advance of a crystal front over time; the reported growth rate was the average of 3 measurements in 3 independent samples. The spontaneous nucleation of FCZ Form I could not be observed in the melt. To study the crystal growth of Form I, a seeding experiment was performed by placing some small FCZ Form I crystals in contact with the sample to initiate the crystal growth.

Raman spectroscopy. The Raman spectra were collected using a Raman microscope (Thermo Fisher DXR, Thermo Fisher Scientific). All samples were irradiated using a 532 nm laser with a 50 μm slit aperture, and Raman spectra were collected by using a 50 X objective with an exposure time of 20 s (1 s × 20 times). Background and fluorescence corrections were applied.

Thermal analysis. Differential scanning calorimetry (DSC) measurements were carried out using a TA Instruments DSC system (TA Instruments, Q2000) equipped with a refrigerated cooling accessory under nitrogen purging (50 mL min^{-1}). Accurately weighed samples (5–10 mg) were loaded in sealed aluminum pans. A pinhole was made in the lid to allow the escape of moisture. The samples were heated at a rate of 10 K min^{-1} to 428 K. The melting point (T_m) corresponded to the extrapolated onset of the melting endotherm. For obtaining the glass transition temperature (T_g) and the recrystallization zone, the samples were melted at 428 K for 3 min, equilibrated to 273 K, followed by reheating at 10 K min^{-1} to 428 K.

Results

Morphologies of FCZ crystals grown from the melts

Fig. 2a and b show the images of FCZ polymorphs grown at 373 K (T_g + 68 K). The spontaneous nucleation rate of Form I in the melt is too slow to observe; thus, the growth of Form I crystals shown in Fig. 2a is initiated by seeding. Form II can spontaneously nucleate from the melt with relatively fast nucleation rates. Form II grows as dumbbell or needle-like crystals from the melt. Confocal Raman microscopy is employed to confirm the polymorphism of FCZ crystals observed in the melt crystallization experiments (Fig. 2c).

The nucleation rate and crystal growth rate of FCZ

Fig. 3a shows FCZ Form II crystals, which nucleate at 303 K over different periods of time (1 and 30 min) and grow at 373 K for 3 min. Only Form II crystals are observed at 373 K on the timescale of measurement. The number of Form II crystals is found to increase with increasing nucleation time. Fig. 3b shows the density of Form II nuclei formed at 303 K as a function of nucleation time. In Fig. 3b, the nucleation of Form II exhibits an induction time of approximately 10 min, followed by a steady-state period where the nuclei density increases linearly with nucleation time. In this work, the nucleation rates are calculated based on the period of steady state.

Fig. 4 shows the nucleation rates and crystal growth rates of FCZ Form I and Form II as a function of temperature. The nucleation rates of Form II are measured between 303 K and 343 K. The maximum nucleation rate of Form II is observed at

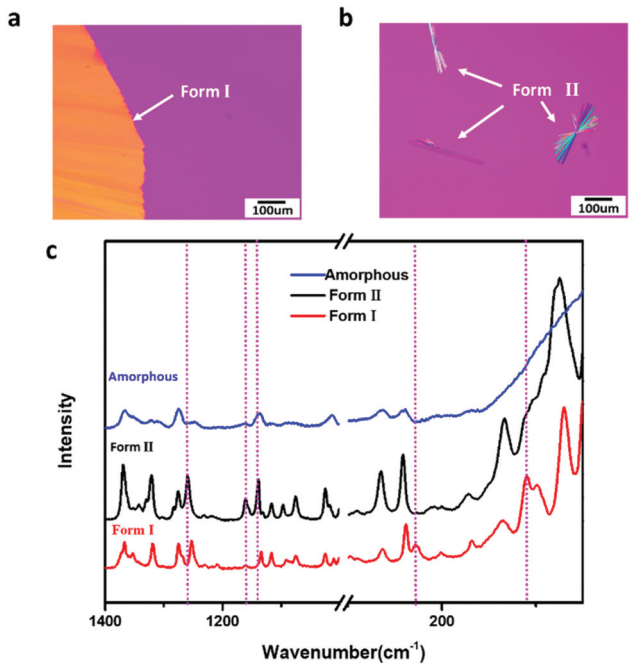

Fig. 2 Polarized optical microscopy images of FCZ polymorphs grown at 373 K, Form I (a) and Form II (b); Raman spectra of amorphous and two polymorphs of FCZ (c) (the dashed lines designate the differences of crystalline and amorphous forms).

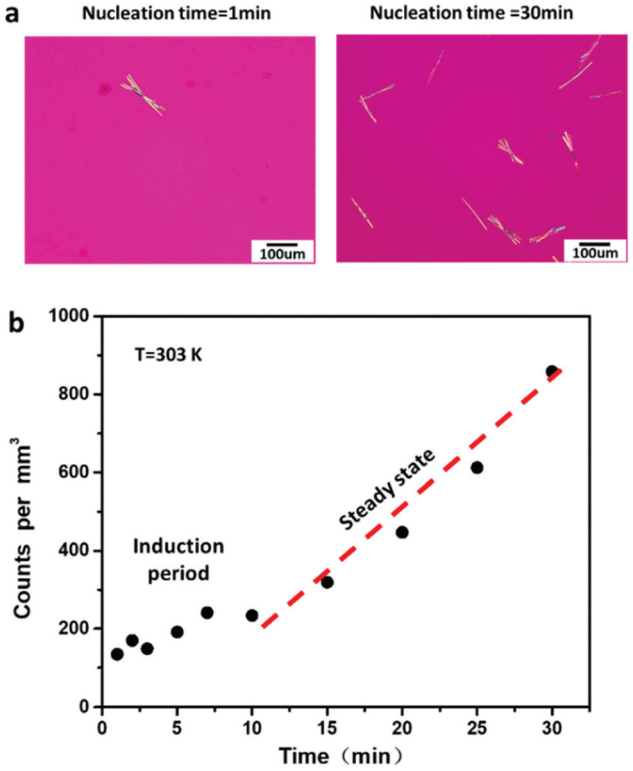

Fig. 3 Two-stage method for measuring nucleation rates in pure FCZ liquid, Form II crystals nucleate at 303 K for 1 and 30 min, followed by 3 min at 373 K (a). Nuclei density as a function of nucleation time at 303 K (b).

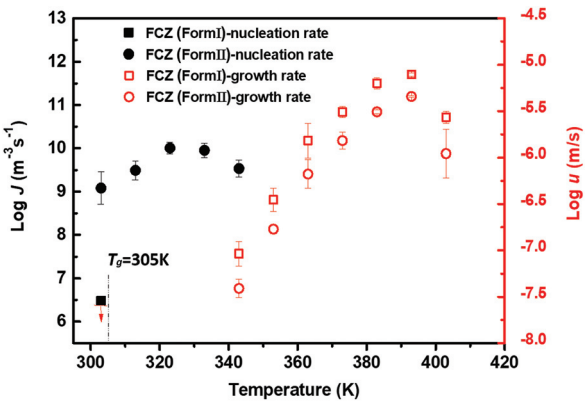

Fig. 4 Nucleation rate and crystal growth rate for amorphous FCZ as a function of temperature (black circles represent the nucleation rates of Form II, black squares represent the estimated upper bound of the nucleation rate of Form I, red empty circles represent the crystal growth rates of Form II, and red empty squares represent the crystal growth rates of Form I) (n = 3).

323 K (T_g + 18 K). However, the nucleation rates of Form I are much slower than those of Form II. No nucleation of Form I was observed over the timescale of our measurements, and an upper bound of the nucleation rate for Form I at 303 K is J = 6.48 m^{-3} s^{-1}. At the same temperature, the nucleation rates of

Form I are projected to be at least 2 orders of magnitude slower than those of Form II. The growth kinetics of two polymorphs between 343 K and 403 K shows a bell-shaped curve, resulting from the competition between thermodynamic and kinetic driving forces for the crystallization.[23,24]

The growth rates of Form I are observed to be slightly faster than those of Form II. The maximum crystal growth rates of Form I and Form II are observed both at the temperature around 393 K (T_g + 88 K). As shown in Fig. 4, the temperature of the maximum crystal growth rate of Form II is well above the temperature of the maximum nucleation rate. Similar temperature-dependent nucleation and growth profiles have been reported in the previous studies.[15,22]

Effect of polymers on the overall crystallization behavior of FCZ by thermal analysis

Thermal analysis was conducted to investigate the impact of polymeric excipients on the overall crystallization behavior of amorphous solids upon heating.[16,25] The DSC traces of amorphous samples are shown in Fig. 5. PVP K30 appears to postpone the onset temperature of crystallization, and the enthalpy of the exothermal crystallization peak decreases with increasing PVP content. No crystallization can be observed in the presence of 30% w/w PVP. The addition of HPMCAS also increases the onset temperature of crystallization. Compared to PVP, HPMCAS exhibits a greater inhibitory effect on the crystallization of amorphous FCZ, as evidenced by no exothermal event that could be detected in the samples with more than 10% w/w polymers. In contrast, the crystallization of amorphous FCZ is accelerated in the presence of PEO. The onset temperature of crystallization decreases with increasing content of PEO (Fig. 5c).

Effect of different types of polymers on the nucleation and crystal growth kinetics of FCZ

Fig. 6a shows the nucleation rates of FCZ in the presence of different types of polymers as a function of temperature. The addition of 10% w/w HPMCAS leads to the largest inhibitory effect on nucleation kinetics, reducing the nucleation rates of Form II by one or two orders of magnitude, while PVP K30 has only a minor inhibitory effect on the nucleation rates of FCZ. In contrast, the nucleation rates of Form II are significantly increased by one or two orders of magnitude in the presence of 10% w/w PEO. Fig. 6b shows the crystal growth kinetics of FCZ Form II with or without adding a 10% w/w polymer. Similar to the effects of additives on the nucleation kinetics, the addition of 10% w/w PEO significantly accelerates the crystal growth rates of FCZ Form II, while HPMCAS and PVP K30 inhibit the crystal growth.

Effect of the polymer content on the nucleation rate and crystal growth rate of FCZ at 343 K

Fig. 7 shows the impact of the polymer content on the nucleation rate and crystal growth rate of FCZ Form II at 343 K. For PVP K30 and HPMCAS, both the nucleation rates and growth rates decrease with increasing polymer concentration. The

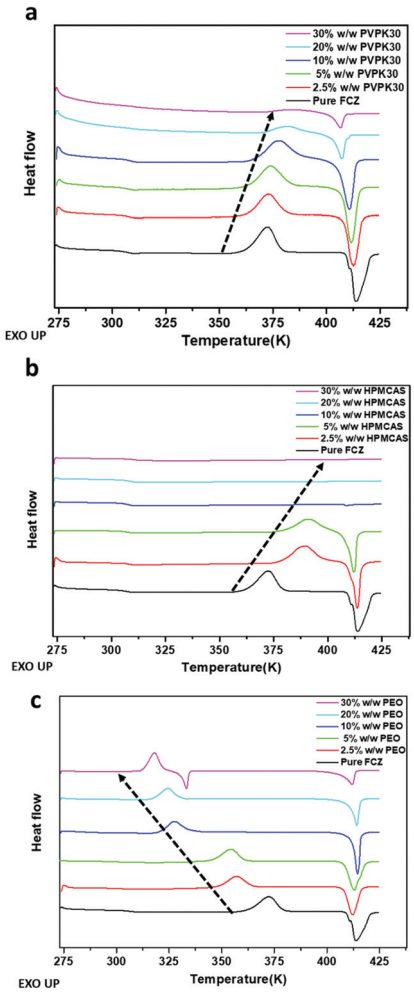

Fig. 5 DSC thermograms of pure amorphous FCZ and amorphous FCZ in the presence of different contents of PVP K30 (a), HPMCAS (b), and PEO (c).

nucleation rates of FCZ Form II decrease more sharply in the presence of HPMCAS than in the presence of PVP K30 with increasing polymer concentration. Conversely, the nucleation rates and crystal growth rates of FCZ Form II increase in the presence of PEO. As shown in Fig. 7c, low-concentration PEO accelerates the nucleation and crystal growth of FCZ Form II to a similar extent.

Effect of the polymer on the nucleation rate and crystal growth rate of two FCZ polymorphs

The nucleation rate of Form I in the absence of polymers is much slower than that of Form II. When FCZ is doped with low-concentration PVP K30 and HPMCAS, no nucleation of Form I could be detected on the timescale of measurement, while Form I can spontaneously nucleate in the presence of 10% w/w PEO and the nucleation rate is significantly increased. As shown in Fig. 8a, the maximum nucleation rate of Form I in the presence of PEO is observed at 313 K (T_g +

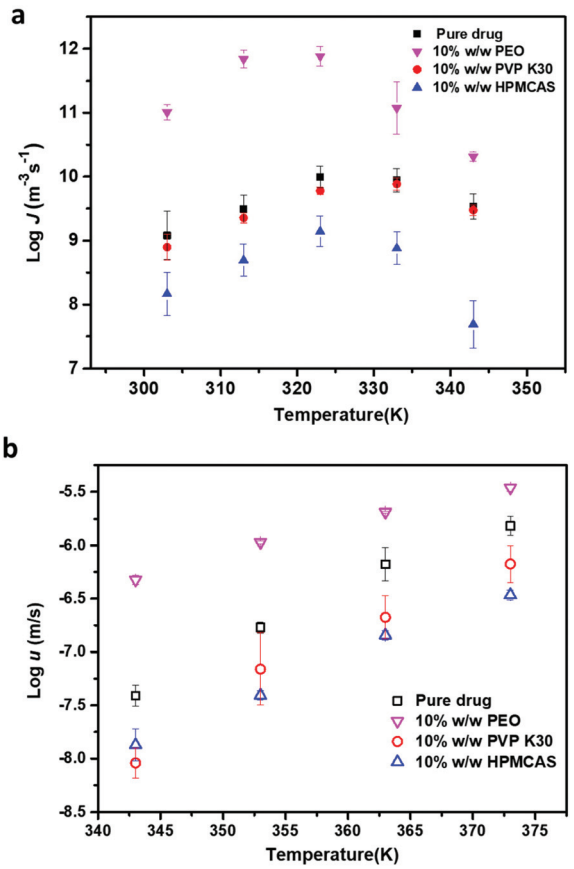

Fig. 6 Nucleation kinetics of FCZ Form II with or without 10% w/w polymers (a). Crystal growth kinetics of FCZ Form II with or without 10% w/w polymers (b) (n = 3).

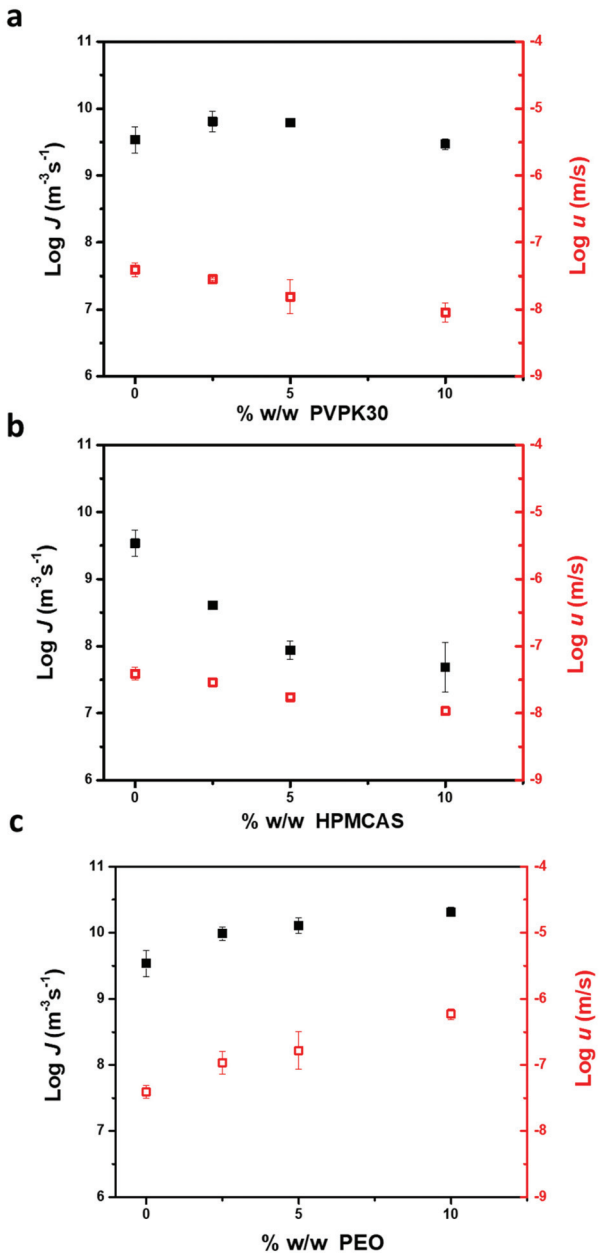

Fig. 7 The nucleation rate and growth rate of FCZ Form II as a function of the polymer concentration at 343 K, PVP K30 (a); HPMCAS (b); and PEO (c) (n = 3).

8 K), slightly below the temperature for the fastest nucleation rate of pure Form II (323 K).

In this work, we also investigated the effect of polymers on the crystal growth kinetics of Form I (Fig. S2†). Similar to the effects of additives on the crystal kinetics of Form II, HPMCAS and PVP K30 inhibit the crystal growth of Form I, while the addition of 10% w/w PEO significantly accelerates the crystal growth rates of Form I. Fig. 8b shows the crystal growth rates of two FCZ polymorphs with or without 10% w/w PEO as a function of temperature. The addition of PEO exhibits a much stronger accelerating effect on Form I than on Form II. A similar phenomenon has been reported and discussed in the previous studies.[10,12,26]

Discussion

The theoretical model of the nucleation rates and growth rates of FCZ Form II from the amorphous state

The classical nucleation theory (CNT) is the most common theoretical model used to illustrate the nucleation kinetics of many systems, such as water,[27] silicate glasses[28] and alloys.[29,30] The CNT has also been used to describe the nucleation of amorphous drugs.[22] According to the CNT, the nucleation rate is expressed as

$$J = k_J \exp(-W_c/kT) \quad (1)$$

where $W_C = \frac{16\pi}{3}\frac{\sigma^3}{\Delta G_V^2}$ is the thermodynamic barrier for forming a critical nucleus, σ is the interfacial energy between the crystal nucleus and liquid, ΔG_v is the energy difference between the crystal and the melt, and k_J is a kinetic factor specifying the attempt frequency at which molecules join the nucleus.

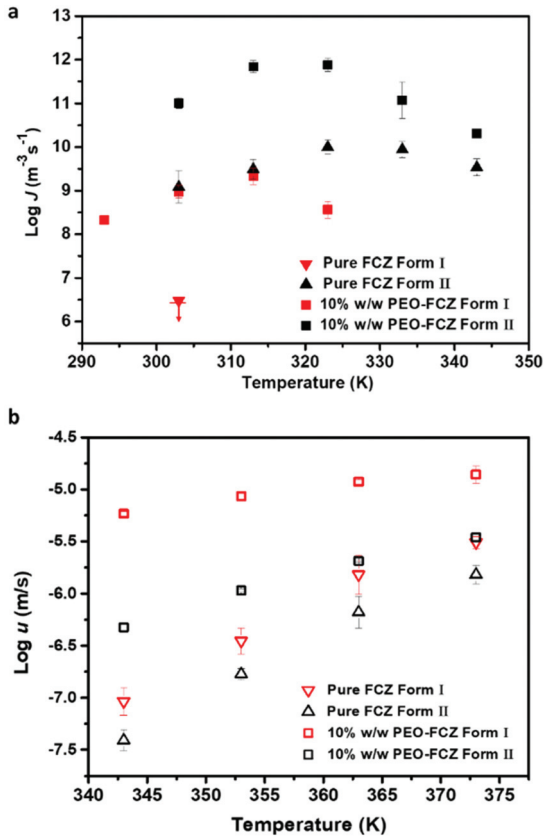

Fig. 8 The effects of 10% w/w PEO on the nucleation rate of FCZ polymorphs at 293–343 K (a) and the crystal growth rate of FCZ polymorphs at 343–373 K (b) (n = 3).

The prefactor k_J can be expressed as a function of measurement of liquid dynamics, such as the diffusion coefficient, viscosity and structural relaxation time.[15] Here, we use viscosity to evaluate k_J,

$$k_J = f_\eta/\eta \quad (2)$$

where η is the viscosity and f_η is a temperature-insensitive constant.

The difference ΔG_v between the crystal and the liquid is calculated from the Hoffman equation,

$$\Delta G_V = \frac{\Delta H_f(T_m - T)T}{T_m^2} \quad (3)$$

where ΔH_f is the heat of fusion and T_m is the melting point.

The viscosity, ΔH_f and T_m of pure FCZ and FCZ doped with polymers are described in the ESI (Tables S2–S4, Fig. S3 and S4†).

Fig. 9 shows the plot of $\ln(J\eta)$ *vs.* $1/(T\Delta G_v^2)$ for Form II in the presence and absence of polymers. As illustrated in Fig. 9, the linear plot suggests that the classical nucleation theory holds in the present systems, and the addition of polymers does not change the nucleation pathway of drugs. Fig. 9 shows that the slopes are negative and the values of crystal–liquid interface energy σ can be calculated from eqn (1) and are listed in Table 1. The values of σ follow the order pure FCZ > PEO-FCZ > HPMCAS-FCZ > PVP K30-FCZ, while the order of the nucleation rate is PEO-FCZ > pure FCZ > PVP K30-FCZ > HPMCAS-FCZ. The different trends of the crystal–liquid interface energy and nucleation rate suggest that the effects of the polymer on nucleation cannot be accounted for by the change of σ.

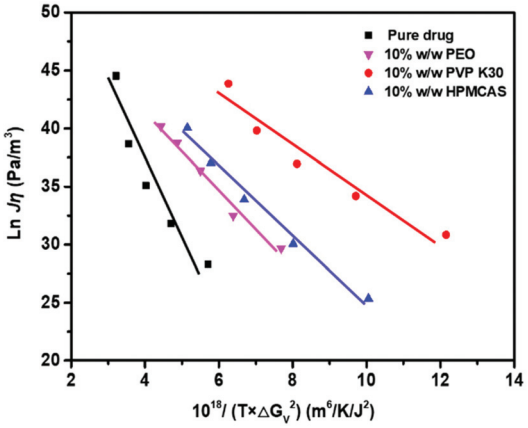

Fig. 9 CNT test for FCZ. $\ln(J\eta)$ is plotted against $10^{18}/(T\Delta G_v^2)$.

Table 1 The interfacial free energies obtained from the CNT fitting in pure FCZ and FCZ doped with polymers

System	σ (J m^{-2})
Pure FCZ	0.017
10% w/w PEO-FCZ	0.014
10% w/w PVP K30-FCZ	0.012
10% w/w HPMCAS-FCZ	0.013

Three theoretical models, including normal or continuous, spiral or dislocation and two-dimensional nucleation, have been used to interpret the crystal growth of glass-forming materials.[22,31] Their common mathematical equation form is described as follows:

$$U = \frac{CTw}{\eta}\left[1 - \exp\left(-\frac{\Delta G_V}{kT}\right)\right] \quad (4)$$

where C is a constant, w is a function of ΔG_v depending on the model of growth, η is the viscosity, ΔG_v is the energy difference between the crystal and the melt, and k is the Boltzmann constant. The term inside the parentheses in eqn (4) is approximately 1 for FCZ.

For growth by two-dimensional nucleation, w in eqn (4) is given by[22,31]

$$w = \exp\left(-\frac{\pi\sigma^2\lambda}{\Delta G_V kT}\right) \quad (5)$$

where λ is the height of the two-dimensional nuclei, and σ and ΔG_v are the same with crystal nucleation. Since λ is unknown, in order to simplify the calculation, we assume that $\lambda^3 = V_{\text{unit-cell}}$. According to the data of the single-crystal structure of FCZ Form II in the literature,[32,33] $V_{\text{FCZ Form II}}$ = 674.05 Å^3; thereby λ equals 8.77 Å.

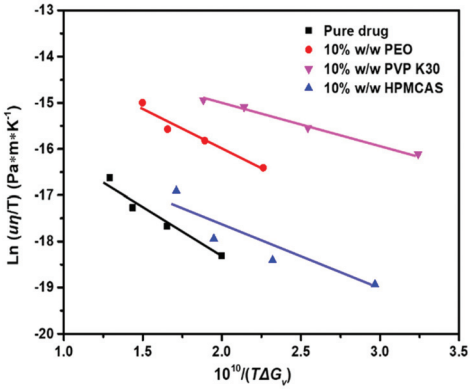

Fig. 10 Two-dimensional nucleation test for FCZ: $\ln(u\eta/T)$ is plotted against $10^{10}/(T\Delta G_v^2)$.

Table 2 The interfacial free energies obtained from the two-dimensional nucleation theory fitting in pure FCZ and FCZ doped with polymers

System	σ (J m^{-2})
Pure FCZ	0.011
10% w/w PEO-FCZ	0.009
10% w/w PVP K30-FCZ	0.007
10% w/w HPMCAS-FCZ	0.009

Fig. 10 shows that the plots of $\ln(u\eta/T)$ *vs.* $1/(T\Delta G_v)$ for pure FCZ Form II and polymer-doped FCZ are linear. The slopes are negative and the crystal–liquid interface energy σ was calculated from eqns (4) and (5), which are presented in Table 2. The value of σ calculated using the growth rates is similar to that obtained from the nucleation data. This further suggests that growth by two-dimensional nucleation takes place for Form II of pure FCZ and FCZ doped with polymers.

Effect of polymers on the nucleation of FCZ

It is of importance to know the effect of excipients on nucleation kinetics of amorphous pharmaceuticals in order to design stable formulations. In this study, three chemically distinct polymers have significantly different effects on the nucleation rates of FCZ. The addition of 10% w/w HPMCAS significantly reduces the nucleation rate of FCZ, while PVP K30 has only a minor inhibitory effect (Fig. 6a). Taylor *et al.* reported that the nucleation of acetaminophen could be significantly decreased by HPMCAS perhaps due to its large monomer unit in comparison with other polymeric additives.[16] Additionally, the drugs containing azole groups have been reported to form strong molecular interactions with HPMCAS.[34–36] Lu *et al.* have quantified the molecular interaction between posaconazole and HPMCAS in ASDs at the angstrom level by using solid-state nuclear magnetic resonance spectroscopy.[35] In another study by Suryanarayanan and co-workers, the molecular mobility of itraconazole was reduced more significantly in the presence of HPMCAS than in the presence of PVP, as evidenced by dielectric spectroscopy.[35] Therefore, the strong inhibitory effect on the nucleation of FCZ by HPMCAS can be attributed to the larger monomer unit and low segmental mobility of the polymer, and strong polymer–drug interactions as well. Unexpectedly, the addition of 10% w/w PEO significantly accelerates the nucleation rate of FCZ. It has been reported that the nucleation rates of felodipine were enhanced by absorbed moisture, and the nucleation rate increased with increasing storage relative humidity.[37] Previously, we found that the highly mobile PEO could act as a plasticizer to accelerate the mobility of amorphous griseofulvin, thus resulting in enhanced crystallization rates.[9,10] Herein, we speculate that the mobility of FCZ molecules could also be accelerated in the presence of PEO, hence promoting the aggregation of molecules to form a critical-sized nucleus.

Many pharmaceutical substances exhibit polymorphism, and additives can alter the crystal growth kinetics of polymorphs.[10,38–40] To the best of our knowledge, the effect of additives on the nucleation kinetics of different polymorphs has never been studied. In this study, the nucleation of Form I is found to be much slower than that of Form II, which is further suppressed in the presence of PVP and HPMCAS. However, the addition of 10% w/w PEO can simultaneously promote the nucleation rates of FCZ polymorphs in the melt. It is reasonable to argue that the addition of PEO increases the molecular collision frequency in the amorphous FCZ system, thus resulting in the enhancement of the nucleation rates for both polymorphs.

Correlation between nucleation and crystal growth kinetics of FCZ in the presence of polymeric additives

The effects of the polymer content on the nucleation and growth rate of FCZ Form II are investigated at 343 K. Fig. 7a and b show that both nucleation and growth rates decrease with the increase of the PVP K30 or HPMCAS content. Fig. 7c shows that the addition of PEO leads to a progressive increase of both nucleation and growth rates by increasing the PEO content. The nucleation and crystal growth rates of FCZ are accelerated to a similar extent in the presence of PEO.

Recently, Yu and co-workers reported the nucleation and crystal growth kinetics of D-sorbitol and D-arabitol doped with low-concentration PVP.[19] They found that J/u is nearly constant, and the nucleation rate in a bicomponent system at a given temperature could be predicted by the following equation:

$$J = (J_0/u_0)u \quad (6)$$

where u is the crystal growth rate of the drug in a bicomponent system at a given temperature T, and J_0 and u_0 are the nucleation and growth rates of a neat drug at T, respectively. The predicted J values of D-sorbitol and D-arabitol are consistent with the observed values, independent of the concentrations or molecular weights of PVP.[19]

In the present work, we also apply the above model to predict the nucleation rates (J values) of FCZ doped with three different polymers. The predicted J values from eqn (6) are plotted against the observed J values of FCZ, and the points

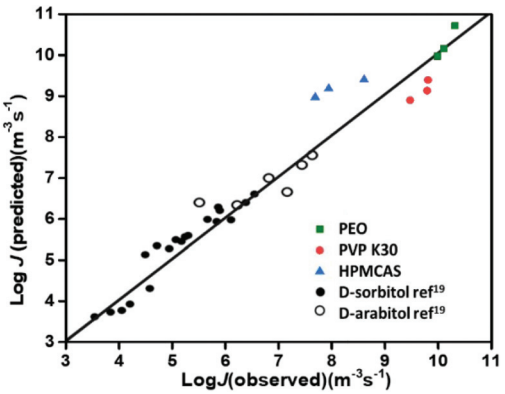

Fig. 11 Observed *vs.* predicted value of nucleation rates in different systems: the plot is reconstructed from ref. 19; PVP-doped D-sorbitol (black circles) and D-arabitol (black empty circles) are from ref. 19; PEO-doped FCZ (green squares), PVP K30-doped FCZ (red circles) and HPMCAS-doped FCZ (blue triangles) are from this work.

are located around the diagonal line (Fig. 11). This plot suggests that the nucleation and crystal growth of FCZ share a similar kinetic barrier, and polymeric additives influence the two processes to a similar extent.[19] However, it is worth noting that there are some deviations for our predicted and observed *J* values, which could arise from the multiple and complicated molecular motions involved in the nucleation and crystal growth processes of multicomponent systems.

Conclusion

In conclusion, we report the effect of polymeric materials on the nucleation and crystal growth kinetics of amorphous fluconazole (FCZ). The nucleation rates of FCZ Form II are significantly inhibited in the presence of 10% w/w HPMCAS. The addition of 10% w/w PVP K30 leads to a minor inhibitory effect on the nucleation rates of FCZ Form II. In contrast, the nucleation rates of FCZ are significantly increased in the presence of 10% w/w PEO. The nucleation kinetics of FCZ could be described by the classical nucleation theory, and crystal growth kinetics fit well into the two-dimensional nucleation growth mode. We propose that the molecular mobilities of amorphous FCZ are either accelerated or decreased by the addition of polymers, hence affecting the aggregation dynamics of molecules for forming the critical sized nucleus. More importantly, the nucleation rates and crystal growth rates of FCZ are found to be influenced by polymers to a similar extent, which suggests that the two processes (nucleation and crystal growth) could share a similar kinetic barrier. This study can aid in selecting appropriate polymeric excipients to formulate amorphous pharmaceuticals with superior stability.

Conflicts of interest

There are no conflicts of interest to declare.

Acknowledgements

The authors are grateful for the financial support to this work from the National Natural Science Foundation of China (No. 81872813), the Outstanding Youth Fund of Jiangsu Province of China (BK20190029), and the Program of State Key Laboratory of Natural Medicines-China Pharmaceutical University (No. SKLNMZZ202031). ZJ thanks the Natural Science Foundation of Jiangsu Province (BK 20200573) and the Project funded by the China Postdoctoral Science Foundation (2020T130139ZX). TC also thanks Prof. Lian Yu (School of Pharmacy, University of Wisconsin, Madison) for helpful discussions.

References

1 L. Yu, *Adv. Drug Delivery Rev.*, 2001, **48**, 27–42.
2 S. V. Jermain, C. Brough and R. O. Williams, *Int. J. Pharm.*, 2018, **535**, 379–392.
3 T. V. Duong and D. M. G. Van, *Opin. Drug Deliv.*, 2016, **13**, 1681–1694.
4 P. Palpandi, B. Raviteja, K. Nagavendra, K. Wahid and S. Mandip, *Int. J. Pharm.*, 2020, **586**, 119560.
5 P. Mistry and R. Suryanarayanan, *Cryst. Growth Des.*, 2016, **16**, 5141–5149.
6 K. Kothari, V. Ragoonanan and R. Suryanarayanan, *Mol. Pharmaceutics*, 2015, **12**, 162–170.
7 A. Newman, *Pharmaceutical.Amorphous Solid Dispersions*, John Wiley & Sons, NJ, 2015, pp. 179–217.
8 A. R. Nair, Y. D. Lakshman, V. S. K. Anand, K. S. N. Sree, K. Bhat and S. J. Dengale, *AAPS PharmSciTech*, 2020, **21**, 309.
9 Q. Shi, C. Zhang, Y. Su, J. Zhang, D. Zhou and T. Cai, *Mol. Pharmaceutics*, 2017, **14**, 2262–2272.
10 Q. Shi, J. Zhang, C. Zhang, J. Jiang, J. Tao, D. Zhou and T. Cai, *Mol. Pharmaceutics*, 2017, **14**, 4694–4704.
11 C. T. Powell, T. Cai, M. Hasebe, E. M. Gunn, P. Gao, G. Zhang, Y. Gong and L. Yu, *J. Phys. Chem. B*, 2013, **117**, 10334–10341.
12 J. Zhang, Q. Shi, M. Guo, Z. Liu and T. Cai, *Mol. Pharmaceutics*, 2020, **17**, 2064–2071.
13 C. Huang, C. T. Powell, Y. Sun, T. Cai and L. Yu, *J. Phys. Chem. B*, 2017, **121**, 1963–1971.
14 D. E. Alonzo, S. Raina, D. Zhou, Y. Gao, G. G. Z. Zhang and L. S. Taylor, *Cryst. Growth Des.*, 2012, **12**, 1538–1547.
15 C. Huang, Z. Chen, Y. Gui, C. Shi, G. G. Z. Zhang and L. Yu, *J. Chem. Phys.*, 2018, **149**, 054503.
16 N. S. Trasi and L. S. Taylor, *CrystEngComm*, 2012, **14**, 5188–5197.
17 T. Miyazaki, Y. Aso, S. Yoshioka and T. Kawanishi, *Int. J. Pharm.*, 2011, **407**, 111–118.
18 H. Konno and L. S. Taylor, *J. Pharm. Sci.*, 2006, **95**, 2692–2705.
19 X. Yao, C. Huang, E. G. Benson, C. Shi, G. G. Z. Zhang and L. Yu, *Cryst. Growth Des.*, 2020, **20**, 237–244.

20 J. E. Kastelic, Z. I. Hodnik, P. Šket, J. Plavec, N. Lah, I. Leban, M. Pajk, O. Planinšek and D. Kikelj, *Cryst. Growth Des.*, 2010, **10**, 4943–4953.
21 A. O. Surov, A. P. Voronin, N. A. Vasilev, A. V. Churakov and G. L. Perlovich, *Cryst. Growth Des.*, 2019, **20**, 1218–1228.
22 V. Andronis and G. Zografi, *J. Non-Cryst. Solids*, 2000, **271**, 236–248.
23 Q. Shi and T. Cai, *Cryst. Growth Des.*, 2016, **16**, 3279–3286.
24 Y. Sun, L. Zhu, T. Wu, T. Cai, E. M. Gunn and L. Yu, *AAPS J.*, 2012, **14**, 380–388.
25 S. T. Niraj and L. S. Taylor, *Cryst. Growth Des.*, 2012, **12**, 3221–3230.
26 J. Zhang, Q. Shi, J. Tao, Y. Y. Peng and T. Cai, *Mol. Pharmaceutics*, 2019, **16**, 1385–1396.
27 G. Bai, D. Gao, Z. Liu, X. Zhou and J. Wang, *Nature*, 2019, **576**, 437–441.
28 V. M. Fokin, E. D. Zanotto, N. S. Yuritsyn and J. W. P. Schmelzer, *J. Non-Cryst. Solids*, 2006, **352**, 2681–2714.
29 S. Karthika, T. K. Radhakrishnan and P. Kalaichelvi, *Cryst. Growth Des.*, 2016, **16**, 6663–6681.
30 A. O. Tipeev, E. D. Zanotto and J. P. Rino, *J. Phys. Chem. B*, 2020, **124**, 7979–7988.
31 I. Gutzow, *J. Cryst. Growth*, 1977, **42**, 15–23.
32 R. C. Mino, A. A. Khouloud and M. O. Rana, *J. Pharm. Sci.*, 2004, **93**, 601–611.
33 M. Karanam, S. Dev and A. R. Choudhury, *Cryst. Growth Des.*, 2011, **12**, 240–252.
34 A. L. Sarode, H. Sandhu, N. Shah, W. Malick and H. Zia, *Mol. Pharmaceutics*, 2013, **10**, 3665–3675.
35 S. P. Bhardwaj, K. K. Arora, E. Kwong, A. Templeton, S. D. Clas and R. Suryanarayanan, *Mol. Pharmaceutics*, 2014, **11**, 4228–4237.
36 X. Lu, M. Li, C. Huang, M. B. Lowinger, W. Xu, L. Yu, S. R. Byrn, A. C. Templeton and Y. Su, *Mol. Pharmaceutics*, 2020, **17**, 2585–2598.
37 H. Konno and L. S. Taylor, *Pharm. Res.*, 2008, **25**, 969–978.
38 U. S. Kestur and L. S. Taylor, *Cryst. Growth Des.*, 2013, **13**, 4349–4354.
39 B. Tian, W. Gao, X. Tao, X. Tang and L. S. Taylor, *Cryst. Growth Des.*, 2017, **17**, 6467–6476.
40 O. Madejczyk, E. Kaminska, M. Tarnacka, M. Dulski, K. Jurkiewicz, K. Kaminski and M. Paluch, *Mol. Pharmaceutics*, 2017, **14**, 2116–2125.